A microRNA signature defines chemoresistance in ovarian cancer through modulation of angiogenesis

Andrea Vecchione[a,b,1], Barbara Belletti[c], Francesca Lovat[b], Stefano Volinia[b,d], Gennaro Chiappetta[e], Simona Giglio[a], Maura Sonego[c], Roberto Cirombella[a], Elisa Concetta Onesti[a], Patrizia Pellegrini[a], Daniela Califano[e], Sandro Pignata[e], Simona Losito[e], Vincenzo Canzonieri[c], Roberto Sorio[c], Hansjuerg Alder[b], Dorothee Wernicke[b], Antonella Stoppacciaro[a], Gustavo Baldassarre[c,2], and Carlo M. Croce[b,1,2]

[a]Division of Pathology and Medical Oncology, Department of Clinical and Molecular Medicine, Faculty of Medicine and Psychology, University "Sapienza," Santo Andrea Hospital, 00100 Rome, Italy; [b]Department of Molecular Virology, Immunology and Medical Genetics and Comprehensive Cancer Center, Ohio State University, Columbus, OH 43210; [c]Division of Experimental Oncology 2, Pathology and Medical Oncology B, Centro di Riferimento Oncologico, Istituto Ricovero e Cura Carattere Scientifico (CRO-IRCCS), 33081 Aviano, Italy; [d]Data Mining for Analysis of Biosystems, Department of Morphology and Embryology, and Medical Oncology, Università degli Studi, 44121 Ferrara, Italy; and [e]Functional Genomic, Pathology and Medical Oncology Units, Department of Uro-Gynecological Oncology, National Cancer Institute, 80121 Naples, Italy

Contributed by Carlo M. Croce, March 26, 2013 (sent for review March 11, 2013)

Epithelial ovarian cancer is the most lethal gynecologic malignancy; it is highly aggressive and causes almost 125,000 deaths yearly. Despite advances in detection and cytotoxic therapies, a low percentage of patients with advanced stage disease survive 5 y after the initial diagnosis. The high mortality of this disease is mainly caused by resistance to the available therapies. Here, we profiled microRNA (miR) expression in serous epithelial ovarian carcinomas to assess the possibility of a miR signature associated with chemoresistance. We analyzed tumor samples from 198 patients (86 patients as a training set and 112 patients as a validation set) for human miRs. A signature of 23 miRs associated with chemoresistance was generated by array analysis in the training set. Quantitative RT-PCR in the validation set confirmed that three miRs (miR-484, -642, and -217) were able to predict chemoresistance of these tumors. Additional analysis of miR-484 revealed that the sensitive phenotype is caused by a modulation of tumor vasculature through the regulation of the VEGFB and VEGFR2 pathways. We present compelling evidence that three miRs can classify the response to chemotherapy of ovarian cancer patients in a large multicenter cohort and that one of these three miRs is involved in the control of tumor angiogenesis, indicating an option in the treatment of these patients. Our results suggest, in fact, that blockage of VEGF through the use of an anti-VEGFA antibody may not be sufficient to improve survival in ovarian cancer patients unless VEGFB signaling is also blocked.

Ovarian cancer is the leading cause of gynecological cancer-related death in the developed world (1). Although progress has been made in its treatment by improved debulking surgery and the introduction of platinum–taxane regimens (2), the overall 5-y survival is only 29% in advanced stage disease (1), mostly because of diagnosis at an advanced stage and intrinsic and acquired resistance to platinum-based chemotherapy. Identifying molecular markers of ovarian cancer chemoresistance is, therefore, of crucial importance. Successful translation of findings at the molecular level will lead to individualized treatment regimens, improved chemotherapeutic response rates, and avoidance of unnecessary treatments.

MicroRNAs (miRs) are a class of small noncoding RNAs that modulate gene expression by causing translational repression, mRNA cleavage, or destabilization (3). They are involved in numerous physiological cellular processes (4–7). Most importantly, accumulating evidence indicates that many miRs are aberrantly expressed in human cancers (8–10), and their expression profiles can classify stage, subtype, and prognosis of some cancers (11–14).

In this report, we describe an miR signature that defines chemoresistant ovarian carcinoma. We show that some miRs are deregulated in most patients with resistant ovarian carcinomas, and we show that miR-484 exerts its action through the regulation of angiogenic factors. We postulate that this miR signature of drug resistance could be used to develop strategies for targeted therapies in chemorefractive ovarian carcinoma patients.

Results

miR Expression in Serous Ovarian Carcinomas is Related to Chemoresistance. To investigate whether miRs could predict serous ovarian carcinoma (EOC) chemoresistance, we analyzed the expression of 676 miRs in the training set (Table S1). As shown in Fig. 1*A*, we were able to identify a response signature with 23 differentially expressed miRs capable of discrimination among the four different groups. Cluster analysis of the centroids (Fig. 1*B*) revealed that the EOC samples can be grouped in two major classes: complete and partial responders. Furthermore, they can be labeled as responders on one side, and stable and progressive disease, labeled nonresponders, is on the other side. Thus, we used these two classes to further refine the response signature and define 12 miRs (Fig. 1*C*). We used 112 EOC samples from a second patient cohort to validate the response miRs (Table S1). Of 12 miRs initially identified, we were able to confirm three miRs down-regulated in nonresponder tumors: miR-484 (P value = 0.0007), miR-642 (P value = 0.041), and miR-217 (P value = 0.046) (Fig. 1*D*). We focused our attention for additional studies on miR-484, which was the most statistically significant.

miR-484 Expression Does Not Alter in Vitro Sensitivity to Carboplatin and Taxol. To obtain insight into the role of miRs in the development of drug resistance, the expression levels of miR-484 were evaluated in six different epithelial ovarian carcinoma cell lines (Fig. S1*A*). Surprisingly, treating the cells for 2 or 4 h with increasing concentrations of carboplatin (CBDCA) and taxol (Tax) showed that their IC_{50} value was not related to the endogenous levels of miR-484, which were evaluated 4 d later by 3-(4, 5-Dimethyl-2-thiazolyl)-2, 5-diphenyl-2H-tetrazolium bromide (MTS) assay (Fig. S1*B*). Moreover, overexpression of miR-484 in both MDAH-2274 and SKOV-3 cell lines did not significantly affect their in vitro sensitivity to CBDCA and Tax (Fig. S1 *C* and *D*).

Author contributions: A.V., B.B., G.B., and C.M.C. designed research; A.V., B.B., F.L., G.C., S.G., M.S., R.C., E.C.O., P.P., D.C., S.P., S.L., V.C., R.S., and A.S. performed research; H.A. contributed new reagents/analytic tools; A.V., B.B., F.L., S.V., G.C., S.G., M.S., R.C., E.C.O., P.P., D.C., S.P., S.L., V.C., R.S., H.A., A.S., G.B., and C.M.C. analyzed data; and A.V., B.B., D.W., and G.B. wrote the paper.

The authors declare no conflict of interest.

Freely available online through the PNAS open access option.

[1]To whom correspondence may be addressed. E-mail: Andrea.Vecchione@osumc.edu or carlo.croce@osumc.edu.

[2]G.B. and C.M.C. contributed equally to this work.

This article contains supporting information online at www.pnas.org/lookup/suppl/doi:10.1073/pnas.1305472110/-/DCSupplemental.

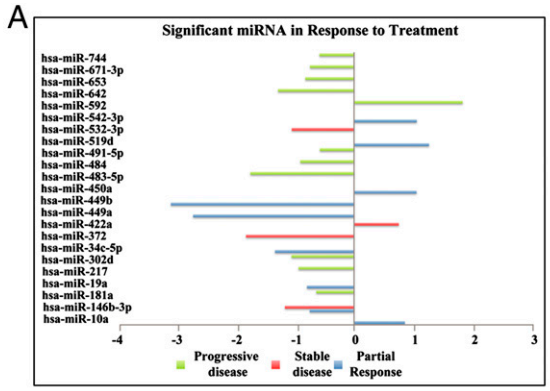

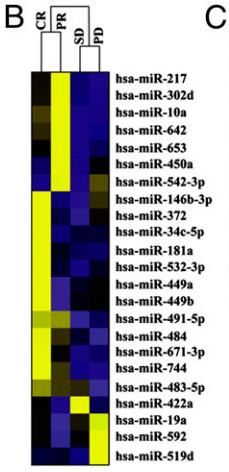

C

miRNAs	Non Responder (3,4) vs. Responder (1,2) (RQ)	(P-Value)
hsa-miR-592	3.0236	0.0003
hsa-miR-484	0.5668	0.0027
hsa-miR-217	0.5149	0.0054
hsa-miR-642	0.465	0.0058
hsa-miR-302d	0.5223	0.0126
hsa-miR-491	0.6721	0.0133
hsa-miR-483-5p	0.3787	0.0159
hsa-miR-653	0.5583	0.018
hsa-miR-181a	0.6965	0.0223
hsa-miR-671-3p	0.6756	0.0244
hsa-miR-19a	1.4148	0.0285
hsa-miR-744	0.7389	0.0412

D

Non Responder (3,4) vs. Responder (1,2)		
miRNAs	(RQ)	(P-Value)
hsa-miR-484	0.5339	0.0007
hsa-miR-642	0.3458	0.041
hsa-miR-217	0.5097	0.0467

Fig. 1. miR signature classifies responder vs. nonresponder ovarian cancer patients. (*A*) Analysis of training set using TLDA cards. Significant miRs in the different classes are shown. Values represent miR fold differences between the groups compared with complete response. (*B*) Centroid analysis of the identified miRs. Blue, down-regulated miRs; yellow, up-regulated miRs. Complete response (CR), partial response (PR), stable disease (SD), and progressive disease (PD) are shown. (*C*) Significant miRs in the training set redefined in two classes: nonresponder (SD and PD) and responder (CR and PR). (*D*) Significant miRs in the validation set. RQ represents fold changes in the two groups.

Role of miR-484 in the Acquisition of Chemoresistance. Because levels of miR-484 were similar among cell lines, we used MDAH-2774 and SKOV-3 cells overexpressing either control miR (scr) or miR-484 to create, in vivo, the responder phenotype and explore the possibility that miRs influence the chemosensitivity of ovarian cancer in a context-dependent manner. miR-484 was stably overexpressed in both cell lines using a lentiviral vector also encoding the EGFP protein to better follow tumor growth in vivo. Stably transduced miR-484 cells showed a 2.0- to 3.5-fold increase in the expression of the miR compared with scr-transduced cells shown in Fig. 5*A*, differences similar to those differences observed in primary EOC between responders and nonresponders tumors. In vitro studies using a fluorescence microscope showed that the EGFP fluorescence was scarcely detectable in MDAH-2774 cells (gray value: 750 ± 120 and 850 ± 230 for MDAH-2774 miR-484 and scr, respectively), whereas it was very bright in SKOV-3 cells, with miR-484 cells slightly brighter than scr-transduced cells (gray value: 5,450 ± 890 and 3,250 ± 630 for SKOV-3 miR-484 and scr, respectively). For these reasons, only SKOV-3 cells were followed for their growth using an in vivo imaging system able to detect the EGFP fluorescence, whereas the growth of MDAH-2774 miR-484 and scr-transduced cells was followed using a caliper-based method.

Cells (1.5×10^6) were inoculated into nude mice s.c. into the left (EGFP-miR-484-MDAH-2774) and right (EGFP-MDAH-2774) flanks and allowed to grow for 15 d. At this time, the tumor volume formed by miR-484–expressing cells was not statistically different from the one observed in control EGFP-expressing cells (Fig. 2*A*, *Left*), indicating that the growth of the primary tumor, at least in the first phases of tumor development, was not affected by the expression of the miR. After CBDCA and Tax treatment, control tumors increased their size about sixfold compared with day 0 at the end of the treatment (range = 2.3–17.7). In the same mice, miR-484–expressing tumors increased only 1.3-fold (range = 0.8–1.8), showing to be much more sensitive to the drugs than the controls (Fig. 2*A*, *Right*). Using an in vivo imaging system able to detect EGFP fluorescence, the analysis of SKOV-3 cells confirmed that the expression of miR-484 did not affect the growth of the primary tumor but significantly increased the sensitivity to treatment (Fig. 2 *B* and *C*). The higher fluorescence intensity of tumors expressing miR-484 in untreated mice (Fig. 2*C*, *Left*) was, in fact, expected, and it reflected the higher EGFP fluorescence intensity of miR-484-SKOV-3 cells observed in vitro. We then used MDAH-2774 cells, which grew more rapidly in nude mice than SKOV-3 cells, to examine whether in vivo administration of the miR could alter the sensitivity of EOC to CBDCA+Tax treatment. Parental MDAH-2774 cells were allowed to grow for 2 wk in the flanks of nude mice, and then, they were injected with lentivirus-expressing EGFP-control miR in the right flank and lentivirus-expressing EGFP-miR-484 in the left flank. Beginning 2 d later, mice were treated biweekly for 3 wk with CBDCA+Tax, and the intratumoral injection of virus was repeated after 1 wk. After 21 d, tumor growth was evaluated. Strikingly, in six of six cases, miR-484 increased drug sensitivity, showing that its expression is able to modulate resistance to CDBCA and Tax in epithelial ovarian cancer in vivo (Fig. 2*D*). To examine the tumor response, mouse samples were stained with H&E, and apoptosis was evaluated by TUNEL assay. Although no increase in apoptosis was observed, it was noted that, in miR-484–transduced tumors, there was a dramatic increase in necrosis. In fact, as shown in Fig. 2 *E* and *F*, miR-484–transduced tumors showed 58.4% ± 17 (range = 27–92), whereas scramble-transduced tumors showed 12% ± 17 (range = 0–65) of necrosis.

miR-484 Regulates the Expression of Angiogenic Factors. Our data pointed to a role of miR-484 in the chemosensitivity of EOC cells in vivo but not in vitro, suggesting that it might act on the tumor microenvironment rather than in a cell autonomous manner. Searching for putative targets, we found that miR-484 may be involved in the regulation of angiogenic factors. In fact, miR-484, according to different prediction algorithms, targets the VEGFB, which is able to directly stimulate endothelial cell growth and migration (15), and the VEGFR2/KDR, which is implicated in all aspects of normal and pathological vascular endothelial cell biology (16). Luciferase and Western blot analyses confirmed that miR-484 overexpression down-regulated the endogenous levels of VEGFB and VEGFR2 (Fig. 3). Thus, we hypothesized that some modifications in the vascular asset of responders and nonresponders in human and mouse tumors might occur. Vascular density was assessed using an antibody against anti-CD34, which is a single-chain transmembrane glycoprotein, associated with human hematopoietic progenitor cells. We used 30 cases of human serous ovarian carcinoma (15 responders and 15 nonresponders) and 28 cases of mice xenograft tumors [14 cases from SKOV-3 and 14 cases from MDAH-2774 (7 cases transduced with miR-484 and 7 cases transduced with EGFP)] and evaluated using the Chalkley eyepiece method (17). In human tumors, the mean microvessel density was 30 ± 1.17 (range = 9–54) for responders and 68 ± 1.6 (range = 15–114) for nonresponders ($P = 0.0000002$); in mice, it was 9 ± 5.5 (range = 1–18) for SKOV-3-miR-484, 23 ± 12 (range = 5–37) for SKOV-3-EGFP ($P = 0.0004$), 10 ± 6.2 (range = 4–22) for

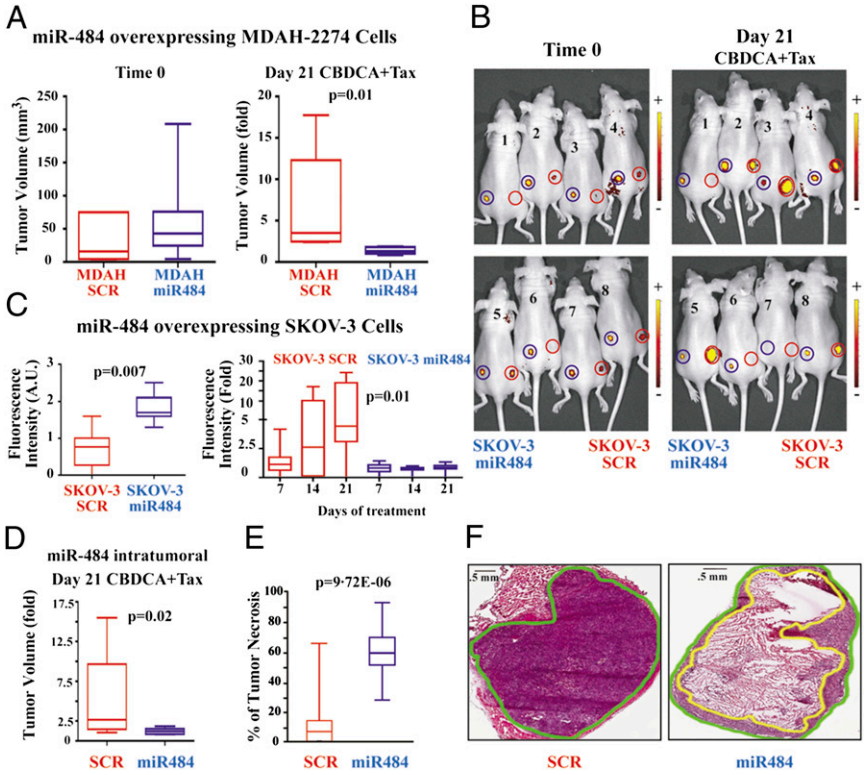

Fig. 2. miR-484 modulates in vivo response to chemotherapy. (*A*) Tumor volume of mice injected in the right flank with MDAH-2774 control cells and injected in the left flank with MDAH-2774–overexpressing miR-484. The size of the tumors (*Left*) at day 0 of the CBDCA+Tax treatment and (*Right*) their increase after 21 d of treatment are shown. (*B*) In vivo imaging of nude mice injected in the right flank with SKOV-3 control cells and injected in the left flank with SKOV-3–overexpressing miR-484. Images were taken (*Left*) immediately before the start of the treatment and (*Right*) after 21 d of CBDCA+Tax treatment. (*C*) Quantification of in vivo EGFP fluorescence of the experiment described in *B* at (*Left*) day 0 and (*Right*) after 7, 14, and 21 d of treatment. (*D*) Effects of intratumoral injection of lentivirus-expressing control (scr) or miR-484 in the presence of CBDCA+Tax treatment. (*E*) Tumor necrosis percentages in scr- and miR-484–transduced tumors are shown. (*F*) H&E examples of (*Left*) scr-transduced tumor and (*Right*) miR-484. Green circles represent the tumor area, and the yellow circle is the area of necrosis. (Scale bar: 0.5 mm.) The significant differences are reported in each graph as evaluated by nonparametric *t* tests. Differences were considered significant when $P < 0.05$.

MDAH-2774-miR-484, and 17 ± 8.9 (range = 5–28) for MDAH-2774-EGFP ($P = 0.0009$) (Fig. 4 *A* and *B*). Performing a Spearman rank correlation test and correlating miR-484 expression values and microvessel density of the same samples, we found a strong inverse relationship between vessel number and miR expression ($r = -0.8$, $P = 1.56E{-}07$), suggesting that the sensitivity of these tumors is caused by their microvessel asset driven by miR regulation (Fig. 4*A*). Accordingly, the expression of VEGFB and VEGFR2 in human tumors correlated with the different levels of miR-484 and the response to therapy. Indeed, responder tumors (high miR-484) showed levels of both VEGFB and VEGFR2 significantly lower than nonresponder tumors (Fig. 4 *C* and *D*) as evaluated by immunohistochemistry. Among 15 responder tumors, 13 tumors expressed weak levels of VEGFB, and 11 tumors expressed weak levels of VEGFR2 (Fig. 4 *C*, *Right* and *D*, *Right*). Conversely, in nonresponder tumors, all but one tumor expressed moderate/high levels of both VEGFB and VEGFR2 (Fig. 4 *C*, *Right* and *D*, *Right*).

miR-484 Is a Secreted miR That Regulates the Expression VEGFR2 in Tumor-Associated Endothelial Cells. Our data indicated, so far, that miR-484 is involved in the regulation of both VEGFB and VEGFR2 in primary ovarian cancers and xenograft tumors formed by ovarian cancer cells (Fig. 4). Although these data compellingly showed that miR-484 targeted VEGFB in EOC cells, we did not observe any effects of miR-484 on VEGFR2 expression in EOC cells, mostly because all of the tested cell lines expressed very low/undetectable levels of the receptor (Fig. 5*E*).

It is now well-accepted that miRs can be secreted and/or released in the local microenvironment and into circulation, acting as paracrine and/or endocrine regulators of several biological functions, including cancer cell growth (18). We, thus, hypothesized that miR-484 could be released into the local microenvironment from EOC cells and penetrate into the endothelial cells, thus eventually modulating its targets. To prove this hypothesis, we first evaluated if miR-484 could be secreted into the conditioned medium of EOC. We evaluated the levels of miR-484 in MDAH-2774 and SKOV-3 cells stably transduced with scr or miR-484 lentiviral vectors in their conditioned medium (CM). Normalized expression of the miR-484 revealed that stably transduced cells showed a two- to threefold increase of its expression over controls (Fig. 5*A*). Importantly, the levels of miR-484 in the CM of SKOV-3 and MDAH-2774 exactly paralleled the miR levels observed in the cells (Fig. 5*B*), showing that miR-484 is secreted and that the amount of miR secreted is directly dependent on the amount of miR-484 produced by cancer cells. Next, we asked whether the secreted miR could penetrate into tumor-associated endothelial cells. We cocultured human umbilical vein endothelial cells (HUVEC) and ovarian cancer cell-derived cell lines overexpressing miR-484-EGFP or scrambled miR-EGFP using a transwell-based assay. HUVEC expressed low levels of miR-484, which were slightly increased by coculture with scrambled miR-EGFP–expressing cells when both SKOV-3 and MDAH-2274 cells were used (Fig. 5*C*). However, levels of miR-484 increased from one- to fivefold compared with controls in HUVEC cells cultured in the presence of

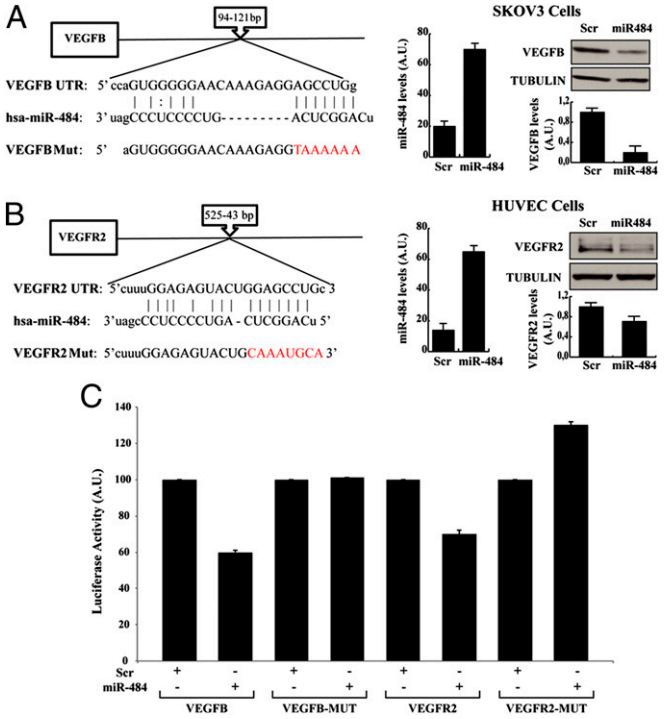

Fig. 3. miR-484 directly targets VEGFB and VEGFR2. (*A*, *Left*) Alignment of potential miR-484 binding sites in the 3′ UTR of VEGFB, (*A*, *Center*) expression of miR-484 in SKOV-3 ovarian cancer cells transfected either with control (scr) or miR-484, (*A*, *Lower Right*) Western blot analysis of VEGFB after transfection of miR-484 in SKOV-3 cells, and (*A*, *Upper Right*) densitometric ratio between the expression of tubulin and VEGFB. (*B*, *Left*) Alignment of potential miR-484 binding sites in the 3′ UTR of VEGFR2, (*B*, *Center*) expression of miR-484 in HUVEC cells transfected with control (scr) or miR-484, (*B*, *Lower Right*) Western blot analysis of VEGFR2 after transfection of miR-484 in HUVEC cells, and (*B*, *Upper Right*) densitometric ratio between the expression of tubulin and VEGFR2. (*C*) Luciferase assay showing decreased luciferase activity in cells cotransfected with pGL3-VEGFB-3′ UTR or pGL3-VEGFR2-3′ UTR and control or miR-484 oligonucleotides. Mutations in the putative miR-484 binding sites, depicted in red in *A* for VEGFB and *B* for VEGFR2, abrogate this effect (Mut). Bars indicate Firefly luciferase activity normalized to Renilla luciferase activity ± SD. Each reporter plasmid was transfected in SKOV-3 cells at least two times (on different days), and each sample was assayed in triplicate.

miR-484–overexpressing cell lines (Fig. 5*C*). In addition, the level of mir-484 in HUVEC cells paralleled the expression of miR-484 in cocultured endothelial cells (compare Fig. 5*A* with Fig. 5*C*). Because the coculture was performed using a transwell-based assay, in which cancer and endothelial cells were separated by a porous membrane, we could exclude that a direct contact between ovarian carcinoma cell lines and HUVEC cells was necessary for the passage of miR-484 from cancer to endothelial cells. Accordingly, incubating HUVEC cells for 24 h only with the CM from miR-484–overexpressing SKOV-3 cells resulted in a twofold increase in the levels of miR-484 compared with controls. To further prove that miR-484 could pass from EOC to endothelial cells when the two types of cells were cocultured, we transfected SKOV-3 cells with a fluorescently labeled miR-484 oligo; 12 h later, cells were washed, detached, and replated in a 1:1 dilution with HUVEC and then cocultured for an additional 24 h. At this time point, cells were fixed and stained with the anti-CD31 antibody to identify the cocultured endothelial cells. As shown in Fig. 5*D*, not only did all of the CD31-negative SKOV-3 cells show the presence of labeled miR-484 in their cytoplasm, but also, 38 ± 10% of CD31-positive endothelial cells were positive for the fluorescently labeled miR-484 (Fig. 5*D*). Collectively, these data show that miR-484 produced from EOC cells is secreted by the neoplastic cells into the local microenvironment and enters HUVEC cells within 24 h. The passage of miR-484 from EOC to endothelial cells had functional consequences: in fact, when HUVECs were cocultured with control and miR-484–overexpressing SKOV-3 cells for 24 h, only the latter cells were able to significantly decrease the expression of VEGFR2 protein on endothelial cells (Fig. 5*E*).

Overall, in vitro and in vivo data show that miR-484 targets both VEGFB and VEGFR2 proteins and suggest that the expression of miR-484 in EOC cells could influence endothelial cell growth and motility in a paracrine manner. To prove this hypothesis, the CM from MDAH-2774 or SKOV-3 cell lines

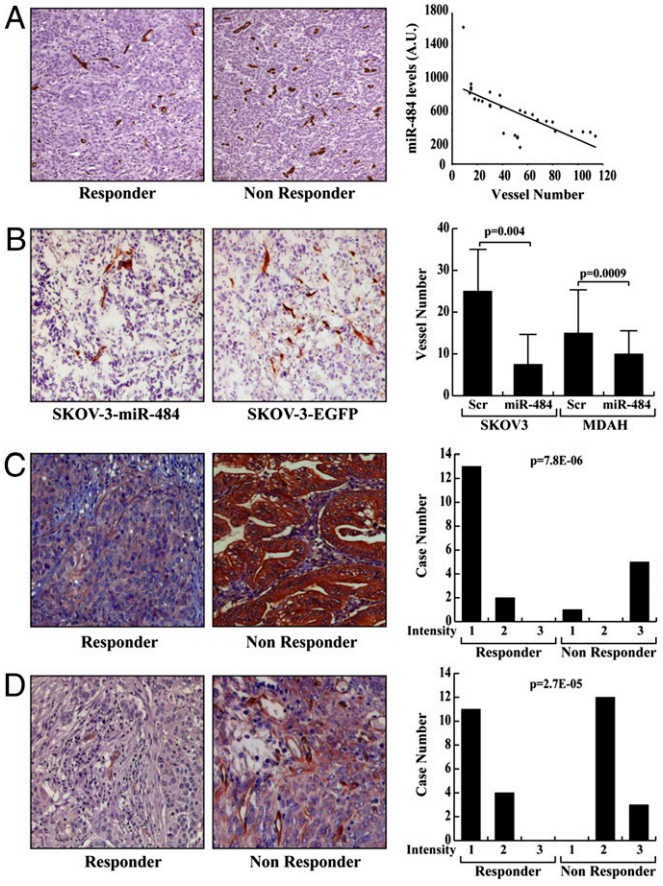

Fig. 4. miR-484 levels correlate with vessel density in ovarian cancer samples. (*A*) Human tumors: CD34 staining (brown) of (*Left*) responder and (*Center*) nonresponder tumors showing a higher vascular density with pronounced microvessel formation in the latter. (*Right*) Regression analysis of miR-484 and vessel number in the same samples. (*B*) Mouse tumors: CD34 staining (brown) of SKOV-3 cell lines xenograft tumors transduced with (*Left*) miR-484 or (*Center*) control (EGFP) showing a higher vascular density in the latter. (*Right*) Tumor vessel count in mouse xenograft tumors transduced with control (EGFP) or miR-484 in SKOV-3 or MDAH-2774 cells. (*C*) VEGFB staining in human tumors: responder tumor showing (*Left*) weak (intensity 1) cytoplasmic VEGFB staining. (*Center*) Nonresponder tumor showing strong (intensity 3) cytoplasmic staining of VEGFB. (*Right*) Case number (*y* axis) and intensity of staining in the different groups (*x* axis). (*D*) VEGFR2 staining in human tumors: responder tumor showing (*Left*) weak (intensity 1) cytoplasmic VEGFR2 staining. (*Center*) Nonresponder tumor showing strong (intensity 3) cytoplasmic staining of VEGFR2. (*Right*) Case number (*y* axis) and intensity of staining in the different groups (*x* axis). The significant differences are reported in each graph as evaluated by nonparametric *t* tests. Differences between groups (responder vs. nonresponder) were considered significant when $P < 0.05$.

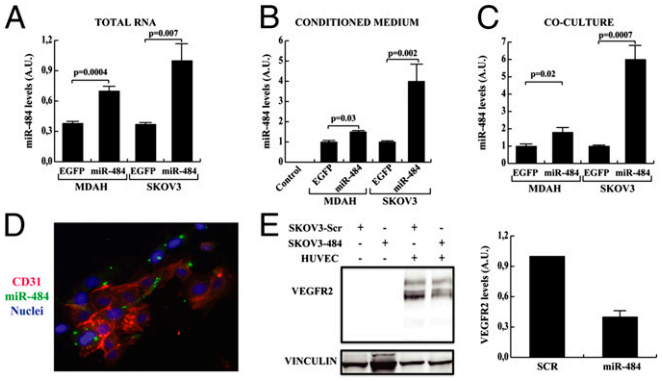

Fig. 5. miR-484 is secreted by ovarian cancer cells and targets VEGFR2 in endothelial cells. (*A* and *B*) Expression of miR-484 in (*A*) ovarian cancer cells and (*B*) their conditioned mediums in cells stably transduced with control or miR-484 vectors. (*C*) Levels of miR-484 in HUVEC cells cocultured with ovarian cancer-derived cell lines. (*D*) Confocal microscopy image of cocultured SKOV-3 cells transfected with miR-484–fluorescin-conjugated (green) and HUVEC stained with CD31 antibody–Texas Red-conjugated (red). (*E*, *Left*) Western blot analysis of VEGFR2 expression in HUVEC cells cultured in CM from SKOV-3 cells stable transfected with miR-484 or EGFP. (*E*, *Right*) Densitometric ratio between the expression of tubulin, and VEGFR2. The significant differences are reported in each graph as evaluated by nonparametric *t* tests. Differences were considered significant when $P < 0.05$.

stably transduced with miR-484 or scr-vector was used to stimulate HUVEC endothelial cells in a tube formation assay on a Matrigel matrix. Video time-lapse microscopy showed that CM, from scr-MDAH-2774 (Movie S1) or SKOV-3 (Fig. S2) cells, was able to induce the formation of tube-like structures when HUVEC cells were cultured for 6 h on 3D Matrigel. This effect was impaired when CM from MDAH-2774– (Movie S2) or SKOV-3–overexpressing miR-484 (Fig. S2) was used and abolished when cells were cultured in the presence of CM for 20 h (Fig. S2). Overall, these data confirm that miR-484 expression in ovarian cancer cells is able to affect the ability of endothelial cells to form and sustain the formation of vascular-like structures.

Discussion

Considering the poor prognosis for patients with ovarian neoplasms, mainly because of late diagnosis and low response to chemotherapy, we have attempted to identify predictive markers of therapeutic response and molecular targets to increase sensitivity to treatment. miRs, a class of gene regulators, have been proven to be effective in classifying normal and cancerous tissues as well as cancer prognosis. Data on ovarian cancer thus far indicate that the miR network is very important to understanding ovarian cancer biology and resistance to therapy (19, 20). Analyzing 198 samples of serous ovarian carcinoma, we discovered that three miRs (484, 642, and 217) were capable of conferring a responder or nonresponder status on ovarian cancer. Focusing our attention on miR-484, we unveiled its mechanism of action in modulating chemosensitivity through the vasculature asset. It is interesting to note that this miR targets both VEGF signaling pathways by either directly modulating the VEGFB protein on the neoplastic cells or interfering with the receptor VEGFR2 in the tumor-associated endothelial cells. The concomitant modulation of the VEGFB and VEGFR2 leads to a normalization of the tumor microenvironment through the control of new vessel formation and maturation, thus improving cancer treatment (21, 22).

Several reports point to the VEGFB–VEGFR1 axis as one of the determinants of ovarian cancer neovascularization (23, 24). The fact that ovarian cancer cells overexpressing miR-484 are less able to stimulate endothelial cell reorganization in vitro (Fig. S2) and neovascularization in mice (Fig. 4) strongly supports this hypothesis. It is also likely that the cooperation between VEGFR1 and -2 signaling is necessary for ovarian cancer growth and drug sensitivity. Indeed, recent results showed that only the simultaneous inhibition of VEGFR1 and -2 is able to significantly reduce the growth of solid human ovarian carcinoma injected i.p. in mice (25).

The importance of neoangiogenesis in ovarian cancer has been proven in human patients, where several phase II clinical trials with antiangiogenic compounds used as single agents to pretreat women resulted in a 16–21% response rate (26). These trials were instrumental for the randomized phase III studies [gynecologic oncology group (GOG) 218 and ICON-7] that compared the added use of bevacizumab with the standard i.v. agents carboplatin and paclitaxel. The results from GOG 218 showed an additional 3.8 mo of progression-free survival (27), whereas the ICON-7 study reported an increased progression-free survival of 1.7 mo (28). Interestingly, the ICON-7 study showed that the benefit of adding bevacizumab to standard chemotherapy particularly benefited patients at high risk of disease progression, supporting our hypothesis that targeting tumor neoangiogenesis will represent a useful approach in the treatment of ovarian cancer patients. However, adding bevacizumab to standard treatment will not represent a cost-effective option for advanced ovarian cancer patients (27). Furthermore, even tumors initially responding to anti-VEGF/VEGFR2 therapy ultimately acquire resistance to the treatment, and relapse occurs in virtually all patients (29). Thus, although antiangiogenic therapy has proven to be a valuable tool in cancer treatment, there is an urgent need for alternative strategies to target the tumor vasculature and better select the patients who will benefit from antiangiogenic compounds. Our work provides important information on both of these aspects and will likely lead to an improved treatment for ovarian cancer patients. In fact, we discovered that the molecular signature of three miRs could potentially identify those patients who will respond to conventional chemotherapy and those patients who will effectively benefit from the addition of antiangiogenic compounds, thereby also reducing the costs of the therapies and improve the efficacy of the drugs. Moreover, our data strongly suggest that blockage of VEGF by the use of an anti-VEGFA antibody alone may not be useful in ovarian cancer patients unless VEGFB signaling is also blocked. Alternatively, small compounds, such as functionalized nanoparticles (30) targeting the VEGFR1 and -2 receptors, could be used as effective therapy in these patients, changing the course of prognosis and treatment of ovarian cancer.

Materials and Methods

A more detailed and complete description of all methods is provided in *SI Materials and Methods*.

Patients. After Institutional Review Board approval (ethical committees of CRO AVIANO, Santo Andrea Hospital and National Cancer Institute, Naples), we obtained 198 specimens of naïve invasive serous carcinoma of the ovary. Data on clinical outcome were obtained from patients' records (Table S1). Response to initial chemotherapy was classified according to the response evaluation criteria in solid tumors (RECIST) guideline as complete response, partial response, stable disease, and progressive disease (31). We randomly divided 198 specimens into a training set of 86 samples and a validation set of 112 samples. All samples were chosen by four pathologists (A.V., S.L., V.C. and A.S.) to minimize the amount of normal tissues (<5%). Where normal tissue exceeded the limitation, we performed laser microdissection of the samples according to standard procedures.

miR Expression Profiling and Data Validation. miR expression profiling was performed on the training set (86 samples) using TaqMan Array Human MicroRNA Set v2.0 containing a total of 676 unique assays. Differentially expressed miRs were validated on the validation set (112 samples) using the TaqMan MicroRNA assay.

Data Analysis. TaqMan Low-Density Array (TLDA) cards and RT-PCR data were analyzed using the comparative CT ($\Delta\Delta C_T$) method (32) for relative

quantification of gene expression on Data Assist ver.1.2 (Applied Biosystems). For each sample, the mean miR expression value was calculated as the average of Ct values smaller than 35. Samples were labeled based on either their response to first chemotherapy or other clinical parameters. We used the one-way ANOVA test to identify differentially expressed miR using R software. Global median normalization was used for the expression analysis of the TLDA cards. miR-16 and -191, both among the most invariable miRs in the training set, were used as endogenous controls for normalization of the RT-PCR in the validation set. All data were expressed as the mean ± SEM. Statistically significant differences between nonresponders and responders (control) were determined using the nonpaired Student two-tailed *t* test. A value of $P < 0.05$ was considered statistically significant. Centroid analysis was performed using Cluster combined with Java TreeView for graphical output. Microarray data have been submitted to the Gene Expression Omnibus (accession no. GSE43867).

ACKNOWLEDGMENTS. This work was supported by Associazione Italiana per la ricerca sul cancro Grant IG 11561 (to A.V.), a grant from Ministero della salute (to A.V. and G.B.), a Centro di Riferimento Oncologico (CRO) Intramural Research Grant (to G.B.), and NIH Grant UO1CA152758 (to C.M.C.).

1. Jemal A, et al. (2008) Cancer statistics, 2008. *CA Cancer J Clin* 58(2):71–96.
2. Bookman MA, et al. (2009) Evaluation of new platinum-based treatment regimens in advanced-stage ovarian cancer: A Phase III Trial of the Gynecologic Cancer Intergroup. *J Clin Oncol* 27(9):1419–1425.
3. Bartel DP (2004) MicroRNAs: Genomics, biogenesis, mechanism, and function. *Cell* 116(2):281–297.
4. Harfe BD (2005) MicroRNAs in vertebrate development. *Curr Opin Genet Dev* 15(4): 410–415.
5. Vecchione A, Croce CM (2010) Apoptomirs: Small molecules have gained the license to kill. *Endocr Relat Cancer* 17(1):F37–F50.
6. Carleton M, Cleary MA, Linsley PS (2007) MicroRNAs and cell cycle regulation. *Cell Cycle* 6(17):2127–2132.
7. Poy MN, et al. (2004) A pancreatic islet-specific microRNA regulates insulin secretion. *Nature* 432(7014):226–230.
8. Volinia S, et al. (2006) A microRNA expression signature of human solid tumors defines cancer gene targets. *Proc Natl Acad Sci USA* 103(7):2257–2261.
9. Petrocca F, et al. (2008) E2F1-regulated microRNAs impair TGFbeta-dependent cell-cycle arrest and apoptosis in gastric cancer. *Cancer Cell* 13(3):272–286.
10. Visone R, et al. (2007) Specific microRNAs are downregulated in human anaplastic carcinomas. *Oncogene* 26:7569–7595.
11. Lu J, et al. (2005) MicroRNA expression profiles classify human cancers. *Nature* 435(7043):834–838.
12. Yanaihara N, et al. (2006) Unique microRNA molecular profiles in lung cancer diagnosis and prognosis. *Cancer Cell* 9(3):189–198.
13. Mattie MD, et al. (2006) Optimized high-throughput microRNA expression profiling provides novel biomarker assessment of clinical prostate and breast cancer biopsies. *Mol Cancer* 5:24.
14. Takamizawa J, et al. (2004) Reduced expression of the let-7 microRNAs in human lung cancers in association with shortened postoperative survival. *Cancer Res* 64(11): 3753–3756.
15. Olofsson B, et al. (1996) Vascular endothelial growth factor B, a novel growth factor for endothelial cells. *Proc Natl Acad Sci USA* 93(6):2576–2581.
16. Olsson AK, Dimberg AD, Kreuger J, Claesson-Welsh L (2006) VEGF receptor signalling - in control of vascular function. *Nat Rev Mol Cell Biol* 7(5):359–371.
17. Suhonen KA, et al. (2007) Quantification of angiogenesis by the Chalkley method and its prognostic significance in epithelial ovarian cancer. *Eur J Cancer* 43(8):1300–1307.
18. Cortez MA, et al. (2011) MicroRNAs in body fluids—the mix of hormones and biomarkers. *Nat Rev Clin Oncol* 8(8):467–477.
19. Dahiya N, Morin PJ (2010) MicroRNAs in ovarian carcinomas. *Endocr Relat Cancer* 17(1):F77–F89.
20. Shih KK, et al. (2011) A microRNA survival signature (MiSS) for advanced ovarian cancer. *Gynecol Oncol* 121(3):444–450.
21. Jain RK (2005) Normalization of tumor vasculature: An emerging concept in anti-angiogenic therapy. *Science* 307(5706):58–62.
22. Escorcia FE, et al. (2010) Selective killing of tumor neovasculature paradoxically improves chemotherapy delivery to tumors. *Cancer Res* 70(22):9277–9286.
23. Delli Carpini J, Karam AK, Montgomery L (2010) Vascular endothelial growth factor and its relationship to the prognosis and treatment of breast, ovarian, and cervical cancer. *Angiogenesis* 13(1):43–58.
24. Sowter HM, et al. (1997) Expression and localization of the vascular endothelial growth factor family in ovarian epithelial tumors. *Lab Invest* 77(6):607–614.
25. Sallinen H, et al. (2009) Antiangiogenic gene therapy with soluble VEGFR-1, -2, and -3 reduces the growth of solid human ovarian carcinoma in mice. *Mol Ther* 17(2): 278–284.
26. Stone RL, Sood AK, Coleman RL (2010) Collateral damage: Toxic effects of targeted antiangiogenic therapies in ovarian cancer. *Lancet Oncol* 11(5):465–475.
27. Cohn DE, Kim KH, Resnick KE, O'Malley DM, Straughn JM, Jr. (2011) At what cost does a potential survival advantage of bevacizumab make sense for the primary treatment of ovarian cancer? A cost-effectiveness analysis. *J Clin Oncol* 29(10):1247–1251.
28. Perren TJ, et al. (2011) A phase 3 trial of bevacizumab in ovarian cancer. *N Engl J Med* 365(26):2484–2496.
29. Bergers G, Hanahan D (2008) Modes of resistance to anti-angiogenic therapy. *Nat Rev Cancer* 8(8):592–603.
30. Liu XQ, Song WJ, Sun TM, Zhang PZ, Wang J (2011) Targeted delivery of antisense inhibitor of miRNA for antiangiogenesis therapy using cRGD-functionalized nanoparticles. *Mol Pharm* 8(1):250–259.
31. Eisenhauer EA, et al. (2009) New response evaluation criteria in solid tumours: Revised RECIST guideline (version 1.1). *Eur J Cancer* 45(2):228–247.
32. Schmittgen TD, Livak KJ (2008) Analyzing real-time PCR data by the comparative C(T) method. *Nat Protoc* 3(6):1101–1108.